July 1998 ● NREL/CP-520-23919

A Wide-Gap a-SiC:H PV-Powered Electrochromic Window Coating

W. Gao, S.H. Lee, Y. Xu, D.K. Benson, S.K. Deb, and H.M. Branz

Presented at the 2nd World Conference and Exhibition on
Photovoltaic Solar Energy Conversion; 6-10 July 1998; Vienna, Austria

National Renewable Energy Laboratory
1617 Cole Boulevard
Golden, Colorado 80401-3393
A national laboratory of the
U.S. Department of Energy
Managed by the Midwest Research Institute
For the U.S. Department of Energy
Under Contract No. DE-AC36-83CH10093

A WIDE-GAP A-SiC:H PV-POWERED ELECTROCHROMIC WINDOW COATING

W. Gao, S.H. Lee, Y. Xu, D.K. Benson, S.K. Deb and H.M. Branz
National Renewable Energy Laboratory,
1617 Cole Blvd., Golden, CO 80401, USA

ABSTRACT: We report on the first monolithic, amorphous-silicon-based, photovoltaic-powered electrochromic window coating. The coating employs a wide bandgap a-$Si_{1-x}C_x$:H n-i-p photovoltaic (PV) cell as a semitransparent power supply, and a $Li_yWO_3/LiAlF_4/V_2O_5$ electrochromic (EC) device as an optical-transmittance modulator. The EC device is deposited directly on top of a PV cell that coats a glass substrate.
The a-$Si_{1-x}C_x$:H PV cell has a Tauc gap of 2.2 eV and a transmittance of 60% to 80% over a large portion of the visible light spectrum. We reduced the thickness of the device to about 600 Å while maintaining a 1-sun open-circuit voltage of 0.9 V and short-circuit current of 2 mA/cm^2. Our prototype 16 cm^2 PV/EC device modulates the transmittance by more than 60% over a large portion of the visible spectrum. The coloring and bleaching times of the EC device are approximately 1 minute under normal operating conditions (±1 volt).
A brief description of photoelectrochromic windows study is also given.
Keywords: a-Si – 1: Wide gap – 2: Electrochromic window – 3

1. INTRODUCTION

A variable-transmittance coating, based on reversibly coloring electrochromic (EC) material, has significant potential applications in architectural windows, the automobile industry, sunglasses, and toys[1,2]. With their ability to modulate solar energy transmittance, EC-coated windows could provide substantial total energy savings considering the worldwide production of flat glass is ~1 billion m^2 per year, and new windows installed in the United States are ~60 million m^2 per year [1,3].

Computer models predict that applications could be highly cost effective when a building's energy management system is constructed from independent, smart components[4]. This system would replace centralized controls with distributed smart components, each reacting to the local environment and energy management requirements. However, the technology presently requires costly low-voltage wiring throughout the building. A monolithic, self-powered tandem PV-EC device would eliminate the need for wiring to each window and should reduce costs[4]. The challenge is to create a window that is easy to manufacture and install, and has sufficient contrast between the bleached and colored states. A semitransparent PV power source distributed over the entire window is a good candidate system.

Electrochromism in transition-metal oxides has been studied extensively since its discovery in 1969[5]. The fundamental mechanism of the change in optical properties remains controversial[6,7]. However, for device engineering a simple phenomenological model suffices. The features of an EC material (e.g., WO_3) that are important for EC-device operation are that (a) a reversible insertion-phase compound is formed with small, mobile ions (e.g., Li^+), and (b) each ion inserted induces an optical absorption center[8,9]. Thus, by inserting and extracting Li^+, the optical absorption of a WO_3 film can be continuously and reversibly varied. Transport of Li^+ in and out of a WO_3 film is balanced by an equal but opposite electron current as given by the reversible reaction:

$$\text{(transparent) } WO_3 + ye^- + yLi^+ \leftrightarrow Li_yWO_3 \text{ (colored)}, \quad (1)$$

which converts transparent WO_3 into optically absorbing Li_YWO_3 and back again. The concentration of Li^+, y, determines the absorption coefficient of the Li_yWO_3 film and thus the optical properties of the darkened EC device. In most EC devices, an ion storage layer (e.g., V_2O_5) undergoes a complementary reaction similar to Equation (1), but there is no corresponding color change. An ion conductor layer (e.g., $LiAlF_4$) ensures that all current flow through the device must be carried by Li^+ ions instead of electrons. The color-state of the complete device is determined by the applied electrostatic potential[10].

The monolithic, tandem PV/EC device (see Fig. 1) requires a transparent PV coating that still outputs enough voltage to drive the EC device and enough current to operate the device at a reasonable speed. For the EC device currently employed, a 25-mC/cm^2 charge is required to finish a darkening or bleaching process. To darken the window in 5 minutes requires only about 0.1 mA/ cm^2 current density from the PV device. This gives room to increase the bandgap and reduce the thickness of a standard terrestrial PV device in order to reach a reasonable bleached-state transparency.

Although there is a considerable body of research on wide-bandgap silicon-carbon alloys, we believe this is the first project to utilize a semitransparent solar cell made entirely of a-SiC:H material[11]. The main technical challenge lies in reducing the thickness to less than 100 nm for semitransparency. When semitransparent PV devices become very thin, the PV device may develop shorts more easily and render the PV/EC stack useless. This problem has made the fabrication of monolithic PV/EC devices challenging.

To realize a monolithic PV/EC structure, each of the nine layers of the tandem device as shown in Fig. 1 (left), our target design, must be optimized to obtain good device performance. In Fig. 1 (left), transparent conducting oxide (TCO) is used for each conducting layer to maximize the device transmittance. By connecting three conducting layers to a battery and controlling circuitry, the device could be fully controlled by the user in the manual mode or automatically controlled by external circuitry. The device can be colored under the light by connecting the top and bottom TCO. When the coloration processes finish, extra energy generated by the PV device could be stored in a rechargeable battery via the middle contact. This energy could be used to bleach the EC device when necessary.

Earlier, we reported side-by-side testing of prototype PV and EC devices[12,13], however, this approach hid some problems we encountered when constructing the monolithic, stacked PV/EC device. Fig. 1 (right) shows the device structure reported here. We used thin gold as the top electrode to save time and improve reproducibility during our preliminary fabrication processes. The middle contact was removed to avoid the PV-shorting problem temporarily. In this way, we are able to stack the PV-EC device together and study the other opto-electronic characteristics of the device.

TCO
WO_3
$LiAlF_4$
$Li_xV_2O_5$
TCO
a-SiC:H-p
a-SiC:H-i
a-SiC:H-n
TCO
Glass

thin Au
WO_3
$LiAlF_4$
$Li_xV_2O_5$
a-SiC:H-p
a-SiC:H-i
a-SiC:H-n
TCO
Glass

Figure 1: Left, target structure of a PV/EC device. The upper half is EC and the lower half is PV. The middle contact permits battery charging and user control. Right, present device structure. When the top and the bottom conductors are connected, the device darkens. An external power is used to bleach the device.

When the device is short-circuited under illumination, the light generates photovoltaic voltage in the PV part, which raises the potential applied to the EC part. This potential difference drives a coloration current through the EC device equal to the current flow through the PV device. To bleach the device, an external voltage is applied between top and bottom electrodes. The bleaching current flows through both the EC and PV portions. In this situation, the PV device is forward biased and presents a small potential barrier that the external power source has to overcome. The size of the barrier is related to the current. At a high bleaching current, this barrier is about same as the open-circuit voltage of the PV device.

In this paper, we report our studies of wide-bandgap semitransparent a-$Si_{1-x}C_x$:H and its incorporation in PV cells, briefly review the EC device characteristics, and describe integration of these devices into a monolithic PV/EC stack. Details of EC device optimization are reported elsewhere[14]. A brief discussion of photoelectrochromic (PEC) device is also given for comparison.

2. EXPERIMENTAL

The PV part of the electrochromic window is fabricated by plasma-enhanced chemical vapor deposition (PECVD) on a smooth SnO_2:F-coated glass substrate, in a single-chamber deposition system. The three layers of the n-i-p solar cell are all made of a-$Si_{1-x}C_x$:H materials. The radio frequency power is between 3 and 6 watts for a 5x5 cm^2 substrate. At approximately 200°C to 220°C substrate temperature and a working pressure of 0.5 to 3 torr, the deposition rate is 1-2 Å/s. Optimized thicknesses of the n, i, and p layers are roughly 10, 40, and 10 nm, respectively. Thicknesses were measured with a Tencor alpha-step 200-step profilometer. Light and dark conductivities were measured using a Keithley 6517A electrometer and an ELH light at 100 mW/cm^2. Following our previous work[12], we define the semitransparency gap, E_{st}, as the photon energy at which the absorption coefficient is $5x10^4$ cm^{-1} (at this energy, approximately half of the photons is absorbed through a 1000-Å film). We calculated E_{st} from optical transmission spectra measured on a Cary 2300 spectrophotometer. The Tauc gap is roughly 0.3 eV below E_{st} in our a-$Si_{1-x}C_x$:H.

The EC part of the electrochromic window is composed of thin-film WO_3 (the electrochromic layer); $LiAlF_4$ (the ion conductor); and V_2O_5 (the ion-storage layer). They are deposited in a thermal-evaporation system by using pure WO_3 powder, a mixture of LiF and AlF_3 powder, and pure V_2O_5 powder, respectively. Their thicknesses are WO_3, 120 nm; $LiAlF_4$, 1000 nm; and V_2O_5, 500 nm. A 55-nm layer of lithium is deposited after V_2O_5 (equivalent to $Li_{1.2}V_2O_5$), and 8.5 nm of gold are used as a semitransparent top contact. The current deposition sequence shown in the Fig. 1 (right) is based on the consideration of preventing the hygroscopic-lithiated $Li_{1.2}V_2O_5$ layer from absorbing water vapor from the air. By properly controlling the layer thickness, the coloring and bleaching voltages are adjusted for compatibility with the underlying PV device. Improvements in transparency would be expected if the Au layer were replaced by a transparent conducting oxide layer. The coloration-cycling measurement were done using a 670-nm laser detected by a photodiode. The hermetic sealing is performed by covering the device with a second glass layer, filling the space with dry nitrogen, and sealing the edges with epoxy.

3. RESULTS AND DISCUSSIONS

3.1 a-SiC:H Material Properties

Extensive research has been reported on amorphous silicon-based wide-bandgap materials, especially on a-$Si_{1-x}C_x$:H[11]. It is well known that the bandgap increases as more carbon is incorporated. Although the amount of carbon incorporated into the film depends on the deposition condition, the relation between optical bandgap and carbon content of a-Si:H material is relatively universal. This had led to the observation that the optical bandgap, E_g, depends linearly on carbon context, x[11],

$$E_g(x)=E_g(x=0)+1.68x, \quad (2)$$

for x between 0 to 0.4. However, as C is added, photoelectronic properties always deteriorate. By hydrogen dilution of the precursor gases, it is possible to make a material that has a bandgap about 0.4 eV greater than a-Si:H while preserving reasonable photoelectronic properties[15].

Fig. 2 shows the optical absorption spectra of films grown with varying C content. E_{st} is successfully adjusted by varying the methane-to-silane ratio in the gas phase during the PECVD deposition. By changing this ratio from 0.67 to 2, E_{st} is increased from 2.25 eV to 2.5 eV (Tauc bandgap from 1.94 to 2.19 eV), equivalent to 10% to 26% of carbon incorporated into the film according to Eqn. (2). Absorption within the spectral region of maximum human eye sensitivity is significantly reduced. If the bandgap were pushed to a higher value, the photoconductivity would be decreased dramatically[11]. In order to keep a reasonable

output from this a-$Si_{1-x}C_x$:H solar cell, the material with 2.5-eV semitransparency gap is used as the i-layer material during our solar cell fabrication. The deposition parameters and measurement results of our chosen material are listed in Table 1.

Table 1: Deposition parameters and properties of the a-$Si_{1-x}C_x$:H intrinsic layer.

SiH_4 (sccm)	CH_4 (sccm)	H_2 (sccm)	Power (mW/cm^2)	P (Torr)	E_{st} (eV)	σ_{ph} (ns/cm)	σ_{ph}/σ_d ($x10^4$)
5	10	75	73	3	2.5	77	18

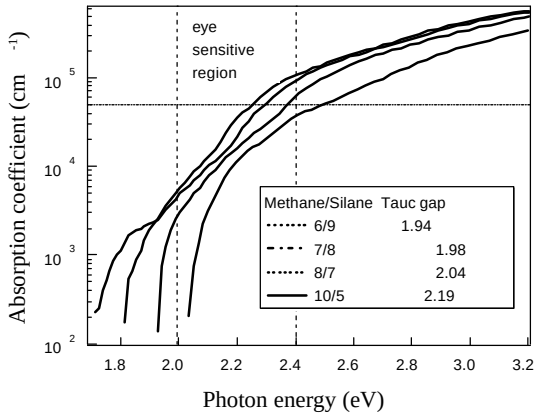

Figure 2: Absorption coefficient curves for the films deposited at different methane/silane ratios.

3.2 PV Device Optimization

To reduce the absorption from the PV portion of the device, one must minimize the thickness of each layer while maintaining a high output voltage to drive the EC device. It is clear that there is a lower limit on device thickness—the best combination of the layer thickness and properties is a compromise between different factors.

A series of thickness-optimization experiments were therefore carried out. The open-circuit voltage (V_{oc}) falls when the p and n layers are thinned beyond a critical thickness. This is due to the weakening of the built-in potential. Our optimized n- and p-layer thicknesses were about 100 Å. The most critical optimization is that of the i-layer. Fig. 3 shows the change of V_{oc}, short-circuit current density (J_{sc}), fill factor (FF), and conversion efficiency of an a-SiC:H solar cell when the i-layer deposition time is reduced from 20 min to 5 min. When the i-layer is less than 40-nm thick, pinholes dramatically degrade the performance of the device. The best results for a PV device at the i-layer thickness of 40 nm are V_{oc}, 0.9 V; J_{sc}, 2 mA/cm^2; FF, 0.5; and efficiency, 1%. This is measured under a Xenon lamp solar simulator

Clearly, I_{sc} and the conversion efficiency are reduced dramatically with the i-layer thickness. However, it is noticeable that the I_{sc} does not change proportionally to the i-layer thickness (I_{sc} is roughly halved when the i-layer thickness changes to 1/4). This shows the effect of improved collection efficiency at higher field intensity inside the i-layer. Another noticeable fact is that V_{oc} decreases from 865 mV at 1600 Å to 741 mV at 400 Å. This phenomenon has previously been reported in crystalline-Si solar cell studies[16,17]. The general trend of V_{oc} change when the device thickness is decreased is determined by the competition of surface and volume recombination. When surface recombination is dominating, V_{oc} will drop with decreasing device thickness, but when volume recombination is dominating, V_{oc} will increase. From this point of view, our device is in a surface- recombination controlled regime even though special attention has been paid to graded buffer layer doping and to interface cleaning during fabrication.

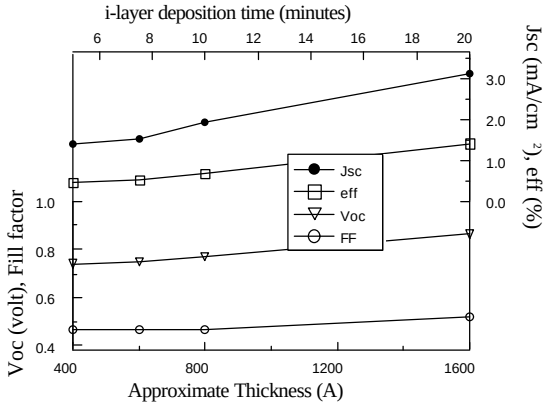

Figure 3: I-V curve parameters of a-SiC:H solar cells versus i-layer thickness.

3.3 EC Device Characterization

Fig. 4 shows transmittance and current density change of an EC test device as a function of time. The device was alternately colored at -1.0 volt and bleached at +1.0 volt. Its transmittance changes between 63% and 20% at 670 nm between the bleached and colored states. At -1 volt (negative bias to the WO_3), the transmittance of the device decreases and approaches its saturation value after 2 min. When the voltage is reversed, the bleaching process finishes in about 1 min. The much shorter bleaching time compared to the coloring process is due to a different Li driving potential. The bleaching-saturation current density is less than 10 $\mu A/cm^2$ due to the low parasitic electronic conductivity of the $LiAlF_4$ ion electrolyte. This device exhibits a good open-circuit optical memory, which is desirable for the present application.

3.4 PV and EC Integration

Fig. 5 shows the transmittance spectra of a 16 cm^2 monolithic PV/EC device with the structure shown in Fig. 1 (right). It is colored by short-circuiting the top and bottom transparent electrodes under 1-sun illumination, and is bleached by applying 2 volts with a polarity that forward biases the PV device. These spectra are shown in the two upper curves of Fig. 5. The bottom curve shows a more deeply colored state obtained by applying 0.6 volt of external coloring voltage to augment the 1-sun PV voltage. Our PV/EC device shows a relative transmittance change of more than 60% at 670 nm under 1-sun illumination, and a 80% change when the small external voltage is applied. The deeper coloration with the external voltage indicates potential to improve the device contrast either by designing for higher PV voltage or by improving the EC device. The absence of a middle conductor in this device required that both coloring and bleaching current flow through the PV and EC device all the time. Therefore, the 2-volt bleaching voltage includes the part required to overcome a built-in potential from the PV device (about 0.8 volt). In the final retrofit electrochromic window structure, a middle contact layer will be inserted for user control and the option of PV battery charging. This effort is ongoing.

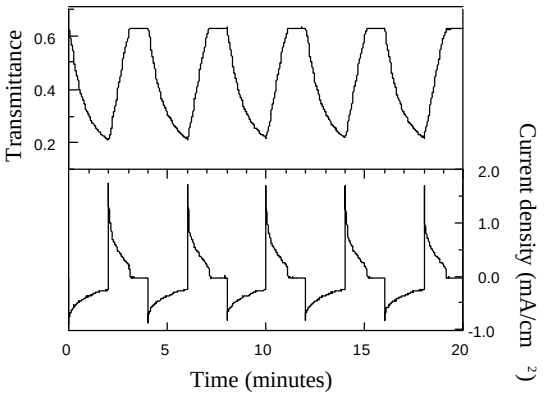

Figure 4: Potentiostatic cycling test measured with a 670-nm laser. Each polarity (±1 volt) is applied for 2 min.

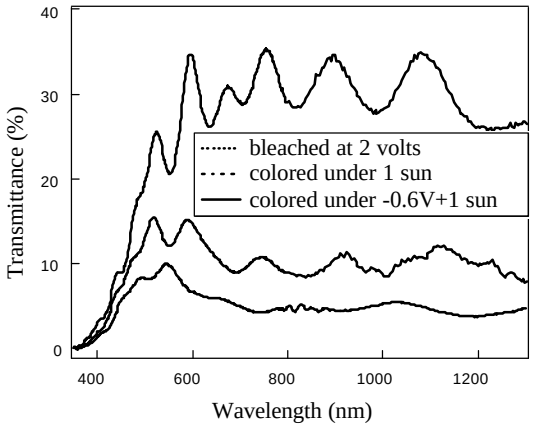

Figure 5: The transmittance spectra of PV/EC device at colored and bleached states under different conditions.

3.5 PEC Windows

NREL has developed an alternative photoelectrochromic device for the self-powered smart window application[18]. The light-absorbing function in the PEC cell is performed by a dye-sensitized semiconductor electrode that produces a photo-voltage sufficient to color the EC film deposited on the counter electrode. A high-surface-area transparent TiO_2 film, consisting of ~30nm-diameter TiO_2 particles sintered at 450°C, is coated with an adsorbed sensitizing dye. Light absorption by the dye leads to electron injection into the TiO_2 followed by re-reduction of the oxidized dye via electron transfer from I^- in solution. The injected electrons move through the TiO_2 film to the contacting SnO_2 electrode and then into the external circuit. The dye coverage was kept low to make the cells almost transparent in the "off" state; The counter electrode was prepared by thermal evaporation of a 500-nm-thick layer of WO_3 onto an indium-tin-oxide coated glass substrate. Cells were fabricated ranging in size from 1 to 25 cm^2.[18].

Self-powered PEC cells have several advantages over the use of conventional photovoltaics for large-area window or display applications. It is a simple device that is easily assembled without electrical shortcircuits. The light–absorbing dye layer can be made optically thin by either reducing the thickness of the TiO_2 layer or by decreasing the concentration of the adsorbed dye. However, because there are only two terminals, there would be less user control compared with the electrochromic window device reported here.

4. CONCLUSIONS

We have made the first monolithic, amorphous-silicon-based, photovoltaic-powered electrochromic window coating. The thickness of the PV device has been reduced to about 600 Å while maintaining 1-sun open-circuit voltage of 0.9 V and short-circuit current of 2 mA/cm^2. The current preliminary design demonstrates most of the features required for a practical, self-powered electrochromic window coating. Design improvements have been identified that could enhance the performance and operational flexibility of the PV/EC coating.

ACKNOWLEDGEMENT

We thank A. Madan and A. Catalano from MVSystems, Inc., for their help in providing a-Si:H deposition facilities and for helpful discussion. This work was supported by OER/BES Advanced Energy Projects of DOE under contract No. DE-AC 36-83CH1009.

REFERENCES

[1] Carl M. Lampert. Solar Energy Materials and Solar Cells **32** (1994) 307.
[2] C.G. Granqvist. Solid State Ionics **53-56** (1992) 479.
[3] S.P. Sapers, et al. 1996 Society of Vacuum Coaters, 39th Annual Technical Conference Proceedings (1996) p 248-255.
[4] D.K. Benson and H.M. Branz. Solar Energy Materials and Solar Cells **39** (1995) 203.
[5] S.K. Deb. Appl. Opt. Suppl. **3** (1969) 193.
[6] S.K. Deb. Philos. Mag. **27** (1973) 801.
[7] R.S. Crandall and B.W. Faughnan. Phys. Rev. Lett. **39** (1977) 232.
[8] B.W. Faughnan, R.S. Crandall and P. Heyman. RCA Review **36** (1975) 177.
[9] R.D. Rauh and S.F. Cogan. J. Electrochem. Soc. **140** (1993) 378.
[10] J.N. Bullock and H.M. Branz. SPIE: Optical Materials Technology for Energy Efficiency and Solar Energy Conversion **2531** (1995) 152.
[11] J. Bullot and M. P. Schmidt. Phys. Stat. Sol. (b) **143** (1987) 345.
[12] J.N. Bullock, C. Bechinger, D.K. Benson, H.M. Branz. J. Non-Cryst. Solids **198-200** (1996) 1163.
[13] C. Bechinger, et al. J. Appl. Phys. **80** (1996) 1226.
[14] S.H. Lee, et al. to be published.
[15] A. Matsuda, et al. J. Appl. Phys. **60** (1986) 4025.
[16] H. Kiess, et al. 11th E.C. Photovoltaic Solar Energy Conference 1992 p. 241.
[17] M.A. Green, et al. 13th E.C. Photovoltaic Solar Energy Conference 1995 p. 13.
[18] C. Bechinger, et al. Nature **383** (1996) 608.